Sex-specific resilience of neocortex to food restriction

Zahid Padamsey[1,2,5], Danai Katsanevaki[2,3], Patricia Maeso[2], Manuela Rizzi[2], Emily Osterweil[2,3,4] and Nathalie L. Rochefort[2, 3, 5]

[1] Wellcome-MRC Institute of Metabolic Science, University of Cambridge, CB2 0QQ, Cambridge, United Kingdom.

[2] Centre for Discovery Brain Sciences, School of Biomedical Sciences, University of Edinburgh, EH8 9XD, Edinburgh, United Kingdom.

[3]Simons Initiative for the Developing Brain, University of Edinburgh, EH8 9XD, Edinburgh, United Kingdom.

[4]Rosamund Stone Zander Translational Neuroscience Center, F.M. Kirby Center, Boston Children's Hospital, Harvard Medical School.

[5]corresponding authors: zp278@cam.ac.uk, n.rochefort@ed.ac.uk

Abstract

Mammals have evolved sex-specific adaptations to reduce energy usage in times of food scarcity. These adaptations are well described for peripheral tissue, though much less is known about how the energy-expensive brain adapts to food restriction, and how such adaptations differ across the sexes. Here, we examined how food restriction impacts energy usage and function in the primary visual cortex (V1) of adult male and female mice. Molecular analysis and RNA sequencing in V1 revealed that in males, but not in females, food restriction significantly modulated canonical, energy-regulating pathways, including pathways associated with AMP-activated protein kinase (AMPK), peroxisome proliferator-activated receptor alpha (PPARα), mammalian target of rapamycin (mTOR), and oxidative phosphorylation. Moreover, we found that in contrast to males, food restriction in females did not significantly affect V1 ATP usage or visual coding precision (assessed by orientation selectivity). Decreased serum leptin is known to be necessary for triggering energy-saving changes in V1 during food restriction. Consistent with this, we found significantly decreased serum leptin in food-restricted males but no significant change in food-restricted females. Collectively, our findings demonstrate that cortical function and energy usage in female mice are more resilient to food restriction than in males. The neocortex, therefore, contributes to sex-specific, energy-saving adaptations in response to metabolic challenge.

Introduction

Mammals reduce their energy usage in times of food scarcity. These adaptations have been well documented for peripheral tissues and are sex-specific. For example, females, as compared to males, readily lose muscle and bone mass to reduce peripheral energy expenditure during food restriction, but lose less fat mass and overall bodyweight[1–6]. Moreover, females are more likely to suppress energy-costly, reproductive functions during food restriction than males, evidenced by substantive reductions in uterine and ovarian mass, as well as a cessation of reproductive function and behaviour[7–9]. Such sex-specific differences are thought to reflect the differential importance of different organs to sex-specific survival[2].

In contrast to peripheral tissue, whether and how the brain adapts its function and energy usage in a sex-specific manner during food scarcity remains largely unknown. The brain requires substantial amounts of energy to process and encode information[10–12]. Indeed, the human brain, which comprises 2% of our body's mass, consumes 20% of our caloric intake, over half of which is used by the cerebral cortex[12]. Previously, we demonstrated that food restriction in male mice reduced energy usage in the primary visual cortex (V1) during visual processing, which was associated with a loss of orientation selectivity and visual coding precision[13]. These changes required a decrease in levels of serum leptin, a hormone secreted by adipocytes in proportion to fat mass[14]. Thus, in males the cortex, like peripheral tissue, has the capacity to reduce its energy usage and function in times of food scarcity.

By contrast, it remains unclear to what extent the brain similarly contributes to energy-saving adaptations during food scarcity in mammalian females. Understanding how food restriction impacts cortical function in males and females is not only of fundamental importance for understanding the sex-specific impact of diet on brain function, but is also critical for studies of cortical function, in which food restriction is used to behaviourally motivate animals[15–17].

Here, we examined how food restriction leading to a 15% loss in body weight over 2-3 weeks impacts energy usage and visual coding in the primary visual cortex (V1) in adult male and female mice. We found that leptin levels, which regulate energy-saving changes in[13], were maintained in females during food restriction, despite being decreased by approximately threefold in males. Consistent with these results, and using a range of experimental techniques, we failed to find significant energy-saving changes in V1 during food restriction in female mice, in contrast to male mice. Specifically, molecular analysis and RNA sequencing of V1 revealed that food-restriction significantly modified canonical energy-regulating cellular pathways in males, but not in females, including pathways associated with AMP-activated protein kinase (AMPK), peroxisome proliferator-

activated receptor alpha (PPARα), and mammalian target of rapamycin (mTOR) signalling, as well as oxidative phosphorylation. Moreover, using *in vivo* ATP and calcium imaging, we found that food restriction significantly reduced V1 ATP usage and orientation selectivity in males, but not in females.

Collectively, our study demonstrates that in times of food restriction, visual cortical function and energy usage are largely maintained in female mice, while they are reduced in males. The neocortex, therefore, contributes to sex-specific, energy-saving adaptations in response to metabolic stress. Our research highlights the importance of taking into account sex differences when studying the impact of dietary manipulations on brain function.

Results

We first examined sex-specific differences in how the neocortex adapts to food restriction in mice. Mice, 7-9 weeks of age, either had *ad libwitum* (CTR) access to food or were food restricted (FR) to 85% of their free feeding bodyweight, for 2-3 weeks (Figure 1A). Prior to any of our recordings, tissue collection, and analysis, all animals were given *ad libitum* access to food until sated. This enabled us to examine the long-term impact of caloric restriction on neocortical function, as opposed to the short-term impacts of hunger[18,19].

Sex-specific impact of food restriction on weight loss and fat mass-regulated hormone leptin

Prior to food restriction, we found that both males and females consumed the same *ad libitum* daily food intake, despite females weighing approximately 80% of age-matched males (weight: male vs. female; 27.82 g [95% CI: 26.84 g – 28.79 g] vs 23.21 g [95% CI: 22.35 g – 24.07 g]; $t = 7.58$; $df = 66$; $p < 0.001$; n = 8 male and 7 female mice). Critically, we found that to achieve a similar magnitude (15%) and rate of weight loss in both sexes we had to impose a 40% greater restriction of daily food intake in females (average of 39% of *ad libitum* intake; n = 7 mice) compared to males (27% of *ad libitum* intake; n = 8 mice) (Figure 1B,C). This is consistent with previous studies demonstrating that female mice are more resistant to weight loss than male[1–6]. Moreover, for similar bodyweight loss (15%) maintained over 2-3 weeks, serum leptin levels, which reflect fat mass, were markedly and significantly decreased (-72%) in males (leptin: CTR male vs FR male; 6.45 ng/mL [95% CI: 4.47 ng/mL – 8.43 ng/mL] vs. 1.84 ng/mL [95% CI: 0.90 ng/mL – 2.79 ng/mL]; $t = 4.58$; $df = 66$; $p < 0.0001$; n = 17 CTR males and 19 FR males), but only modestly and non-significantly decreased (-28%) in females (leptin: CTR females vs FR females; 3.94 ng/mL [95% CI: 2.53 ng/mL – 5.35 ng/mL] vs. 2.83 ng/mL [95% CI: 1.20 ng/mL – 4.47 ng/mL]; $t = 1.00$; $df = 66$; $p = 0.32$; 23 CTR females and 11 FR females) (Figure 1D). This is in keeping with previous findings that female mice are more resistant to fat loss than

98 males[1–6] and that weight loss arises from other tissues including those associated with reproductive
99 functions (ovarian and uterine mass)[7–9].
100
101 **Cellular energy-regulating pathways in cortex are significantly impacted by food restriction in males**
102 **but not in females**
103 Decreased leptin levels are necessary for triggering energy-saving changes in the mouse visual cortex
104 during food restriction[13]. We therefore asked whether the absence of significant change in serum
105 leptin in food-restricted females was associated with any change in V1 energy usage. We first assessed
106 this at the molecular level by examining AMPK phosphorylation state. AMPK is a canonical cellular
107 energy sensor activated by metabolic stress - such as food restriction, in part via decreased leptin
108 signalling - through phosphorylation of threonine 172 (Thr^{172})[20–22]. Its activation results in reduced ATP
109 expenditure, for example, through the inhibition of mammalian target of rapamycin (mTOR)
110 signalling[20,23], and regulation of mitochondrial oxidative phosphorylation[24,25]. In V1, we found that
111 AMPK Thr^{172} phosphorylation was markedly and significantly elevated (2.9 fold) with food restriction
112 in males (AMPK Thr^{172} phosphorylation: CTR male vs FR male; 13.19 AU/µg [95% CI: 7.68 AU/µg – 18.71
113 AU/µg] vs. 38.21 AU/µg [95% CI: 16.50 AU/µg – 59.93 AU/µg]; t = 2.28; df = 39; p = 0.022; n = 11 CTR
114 males and 15 FR males), consistent with ATP savings, but only modestly increased (1.4 fold) in females;
115 this increase was not statistically significant (AMPK Thr^{172} phosphorylation: CTR female vs. FR female;
116 20.94 AU/µg [95% CI: 9.42 AU/µg - 32.46 AU/µg] vs. 29.52 AU/µg [95% CI: 8.52 AU/µg – 50. 53 AU/µg];
117 t = 0.64; df = 39; p = 0.11; 11 CTR females, and 6 FR females) (Figure 1E). We also examined the activity
118 of peroxisome proliferator-activated receptor alpha (PPARα), which is downstream of leptin signalling
119 and is known to regulate fatty acid metabolism and energy homeostasis[22,26]. As with AMPK, we found
120 that PPARα was significantly regulated by food restriction selectively in males, but not in females
121 (Figure 1E)[27,28].
122 To further investigate how energy-regulating cellular pathways are impacted by food
123 restriction, we performed RNA sequencing on tissue dissected from V1 (Figure 2A; n = 4 CTR male, n
124 = 4 FR male, n = 4 CTR female, and n = 4 FR female mice). Differential gene expression analysis using
125 DESeq2 revealed that food restriction significantly altered the expression of 657 and 585 targets in
126 males and females, respectively (at a threshold of p-adj $\leq$ 0.1; only 125 of these were common to both
127 sexes (Figure 2B). To assess the functional relevance of the transcriptomic changes induced by food
128 restriction, we performed Gene Set Enrichment Analysis (GSEA) to identify pathways enriched in the
129 differentially expressed populations. We found that food restriction resulted in a significant alteration
130 of 34 and 14 gene sets (at p-adj $\leq$ 0.05) in males and females respectively; 13 of these were common
131 to both sexes (Figure 2C; Table 1; Table 2). In male mice, we specifically found that food restriction

132 significantly regulated gene sets associated with canonical energy-regulating pathways (Figure 2),
133 including those associated with oxidative phosphorylation and mTOR signalling (mTORC1 signalling
134 and PI3K/AKT/mTOR signalling), as well as fatty acid metabolism; these pathways are known to
135 regulated by leptin and AMPK signaling[20,27–29] (Figure 2D). Notably, these pathways were not
136 significantly regulated by food-restriction in females. In addition to these findings, we found that gene
137 sets associated to estrogen-regulating pathways were significantly regulated in food-restricted males
138 and not in females (Figure 2C). This is consistent with previous findings showing that estrogen, like
139 leptin, suppresses food intake and promotes energy expenditure[30]. Finally, consistent with past
140 studies in cortex, we found that food restriction in males altered gene expression associated with
141 inflammation and reactive oxidative species (Figure 2D)[31,32].
142 Collectively these findings reveal that food restriction strongly affects energy-regulating
143 cellular pathways in the cortex of male, as opposed to female, mice.
144
145 **ATP usage in V1 is significantly decreased under food restriction in males but not in females**
146 We next examined energy usage in visual cortex during visual processing using two photon ATP
147 imaging in V1 of awake, head-fixed Thy1-ATeam1.03^{YEMK} mice, which express a FRET-based ATP
148 sensor[33,34] (Figure 3A). In the presence of ATP synthesis inhibitors, focally applied over the visual
149 cortex, ATP usage can be seen as a decay of the FRET signal during visual stimulation with natural
150 stimuli[13] (Figure 3A). Data obtained in females were compared to our previously published datasets
151 obtained under similar conditions in male mice[13]. As previously shown[13], food restriction robustly
152 decreased the rate of cortical ATP usage in males (24% decrease) (half-time of FRET decay: CTR male
153 vs. FR male; 8.48 min [95% CI: 7.59 min – 9.37 min] vs. 10.51 min [95% CI: 9.08 min – 11.93 min]; t =
154 2.87; df = 37; p = 0. 0067; n = 11 CTR males and 10 FR males) during visual stimulation; a more modest
155 trend was observed in females (12% decrease), which was not significant compared to controls (half-
156 time of FRET decay: CTR female vs. FR female; 8.66 min [95% CI: 7.49 min – 9.84 min] vs. 9.66 min
157 [95% CI: 8.92 min – 10.39 min]; t = 1.36; df = 37; p = 0.18; n = 12 CTR females and n = 8 FR females)
158 (Figure 3B-C). In the absence of visual stimulation (darkness), ATP usage was lower than during visual
159 stimulation and unaffected by food restriction, for either sex (Supplemental Figure 1).
160 Altogether, these findings demonstrate that food-restriction significantly impacts V1 energy
161 usage during visual stimulation in males but not in females.
162
163 **Orientation selectivity in V1 is significantly reduced under food restriction in males but not in**
164 **females**

We next examined how food restriction impacts visual cortical function. In male mice, reductions in energy usage in V1 during food restriction are associated with a decreased visual coding precision as evidenced by a reduction of orientation selectivity[13]. Given the non-significant impact of food-restriction on energy usage in female mice, we reasoned that orientation selectivity would also be less impacted. We analysed two-photon calcium imaging data of V1 GCaMP6s-labeled layer 2/3 neurons in female mice viewing drifting gratings (Figure 3D-F; n = 7 CTR male, n = 8 FR male, n = 7 CTR female, and n = 9 FR female mice). Data obtained in females were compared to our previously published datasets obtained under similar conditions in male mice[13]. Consistent with our hypothesis, in contrast to males in which orientation selectivity was significantly reduced by 27% (OSI: CTR male vs. FR male; 0.58 [95% CI: 0.51 – 0.65] vs. 0.42 [95% CI: 0.36 – 0.49]; t = 3.75; df = 27; p = 0.0009), orientation selectivity was modestly (13%) and not significantly reduced by food-restriction in females (OSI: CTR female vs. FR female; 0.60 [95% CI: 0.52 – 0.67] vs. 0.52 [95% CI: 0.45 – 0.58]; t = 1.90; df = 27; p = 0.08) (Figure 3E-F). Direction tuning, as measured by the direction selectivity index (DSI) was also significantly affected by food-restriction in males, but not in females (Supplemental Figure 3; Males: CTR vs. FR; t = 2.16; p = 0.023; df = 12; n = 6 CTR males and 8 FR males; Females: CTR vs. FR; t = 1.49; p = 0.16; df = 14; n = 7 CTR females and 9 CTR females).

Altogether, our results show that energy usage and coding precision in the visual cortex are largely maintained in female mice under food restriction while they are robustly reduced in males. Such findings cannot be readily attributed to differences in behavioral or attentional state. All animals were imaged whilst in a cardboard tube, and therefore not locomoting. Moreover, we found no difference in pupil size during the presentation of visual stimuli (Supplemental Figure 2).

Bayes factor analysis reveals statistically robust impact of metabolic stress on V1 energy usage and visual coding in males, but not females

We used Bayes factor hypothesis testing to better assess the statistical impact of food restriction on visual cortical function and energy usage in male and female mice (Supplemental Figure 3). Bayes factor analysis uses a Bayesian framework to quantify how much more likely the data is under the alternative hypothesis (*i.e.* there is an effect of food restriction) versus the null hypothesis (*i.e.* there is no effect of food restriction), quantified by the Bayes factor (BF_{10})[35,36]. A $BF_{10} > 3$, for example, means that the data are >3 times more likely under the alternative hypothesis than the null hypothesis. Critically, the BF_{10} allows for a more informative comparison of the effects of food restriction between sexes, as opposed to comparing p-values, which can be misleading[35,36]. Across the parameters of energy usage and visual coding that we tested (Figures 1-3), BF_{10} for males was consistently several-

199 fold greater than that for females. Thus, visual cortical function and energy usage was more robustly
200 modulated by food restriction in males than in females.

201 Our findings however cannot rule out a potential, smaller impact of food restriction on cortical
202 function and energy usage in females, below the threshold for statistical detection in this study. In
203 particular, for females, we found only 3 out of the 10 parameters had $BF_{10} < 0.33$, *i.e.* the data are 3
204 times more likely under the null hypothesis than the alternative hypothesis supporting the absence of
205 an effect [35,36](Supplemental Figure 3). This suggests that food restriction may have a modest impact
206 on V1 energy usage or function in females, but below the limits of statistical detection in our study.

207 Altogether, our results show that energy usage and coding precision in the visual cortex are
208 largely maintained in female mice under food restriction while they are robustly reduced in males.
209

210 Discussion

211 Here, we find that in female mice, energy usage and visual coding in V1 is largely unchanged under
212 food restriction. Using molecular analysis and RNA sequencing, we found that energy-regulating
213 pathways were not significantly changed with food restriction in females, in contrast to males; these
214 included pathways associated with AMPK, mTOR, and PPARα signalling, as well as oxidative
215 phosphorylation. Consistent with this, we found that food restriction in females did not impact visual
216 cortical ATP usage nor orientation selectivity, both of which were reduced by food restriction in males.
217 Our findings suggest that the contribution of neocortex to energy-saving adaptations during food
218 restriction is sex-selective and more pronounced in males; females may rely on other energy-saving
219 strategies, such as reducing reproductive function, to cope with food restriction.

220 *Limitations of the study*

221 Our study focused on the effects of a moderate food restriction protocol over 2-3 weeks on neocortical
222 function and energy usage. This protocol is widely used in metabolic studies investigating the impact
223 of caloric restriction on peripheral physiology, as well as in neuroscience studies to motivate rodents
224 to perform specific behaviors[6,15–17]. However, it remains unclear to what extent our findings generalize
225 to other protocols of food restriction. Indeed, the duration, magnitude, and pattern of food restriction,
226 as well as macronutrient composition are known to impact the physiological responses to dietary
227 manipulations[22,37–39]. Moreover, whilst we focussed our study on the adult visual cortex, it remains
228 unclear if the brain shows similar sex-specific energy-saving adaptations in other cortical areas, and
229 how such adaptations change with age[6,40].

230 A key strength of our study is that we consistently found, across a number of experimental
231 methods, that changes in cortical function and energy usage were significant in males, but not in

232 females. However, a critical limitation of our study is that we did not have the statistical power to
233 directly compare the effect size of food restriction between the sexes (e.g. ANOVA interaction effects);
234 to do so would require a substantial increase in experimental group sizes by several fold. We
235 addressed this limitation, in part, using Bayes factor analysis, which revealed that the impact of food
236 restriction in males was indeed more robust than in females. This analysis also revealed that our study
237 did not have sufficiently strong evidence to definitively rule out a smaller effect of food restriction in
238 females, which may not have been statistically detectable.

239 ***Role of leptin and sex hormones in food restriction impact on cortical activity***

240 Consistent with past studies, we found that food-restricted female mice resisted weight loss, and
241 therefore required a greater restriction of food to achieve similar weight loss (relative to baseline) as
242 males. In addition, for the same relative weight loss as males, females exhibited minimal reductions
243 in serum leptin levels (secreted by adipocytes), consistent with past studies showing that females
244 resist fat loss during food restriction[1–3,5,6]. Similar effects have been observed across several
245 mammalian species, including humans, and is thought to reflect the differential importance of fat
246 stores for reproductive success in males and females[1–5]. Notably, we previously demonstrated that
247 reductions in leptin levels during food restriction are necessary for driving energy-saving changes in
248 visual cortical coding in male mice; leptin therefore acts as a critical signal linking the neocortex to fat
249 stores[13]. That leptin levels are not significantly affected by food restriction in females may explain the
250 minimal impact food restriction has on cortical energy usage and coding precision in female mice.

251 In addition to leptin, sex hormones likely contribute to sex-specific adaptations to food
252 restriction[41]. As with leptin, estrogen suppresses food intake and promotes energy expenditure[30], in
253 part by augmenting leptin signalling by increasing leptin-induced phosphorylation of STAT3[42].
254 Moreover, estrogen can enhance ATP production by sensitizing insulin signalling, enhancing glycolysis
255 and oxidative phosphorylation, and along with progesterone, upregulating mitochondrial gene
256 expression and function[30,43,44]. Interestingly, in our study, RNA sequencing revealed that estrogen
257 signalling pathways were significantly regulated in male visual cortex with food-restriction, and were
258 unchanged in females. Estrogen may thus have overlapping effects with those induced by food
259 restriction, thereby diminishing further responses to food restriction in females[6]. Notably, it was
260 recently shown that sex differences in calorie-restriction's metabolic effects that are observed in
261 young adult mice, are largely absent in older mice, when females' estrogen levels have declined[6].
262 Further studies will be needed to explore whether the resilience of cortical function found in this study
263 in young cycling adult females is also observed in non-cycling mice with reduced oestrogen levels, such
264 as in aged mice.
265

266 ***Sex-specific regulation of cellular energy-regulating pathways***

267 AMPK and mTOR signalling pathways are canonical regulators of cellular energy usage[20,23]. We found
268 these pathways, along with cortical ATP usage, to be significantly modulated by food-restriction in
269 male, but not female mice. AMPK is activated during metabolic stress, and saves energy by regulating
270 oxidative phosphorylation[24,25], and inhibiting cellular pathways associated with energy usage, such as
271 mTOR signalling[20]. mTOR signalling, by upregulating protein synthesis, increases ATP usage by
272 promoting neuronal excitability, neurite outgrowth, ion channel expression, and synaptic plasticity[23].
273 mTOR signalling is therefore ideally situated to regulate how much ATP is used in neuronal function;
274 its inhibition may underlie ATP savings and the associated loss of coding precision with food-restriction
275 in male mice. Notably, previous studies have found sex- and tissue- dependent regulation of AMPK
276 and mTOR signalling, including in response to food restriction[41]. For example, in skeletal muscle, mTOR
277 signalling is enhanced by fasting selectively in male, but not female mice[41,45]. Moreover, metabolic
278 challenge by endurance training induces greater AMPK activity in cardiac tissue in male, as opposed
279 to female mice[46]. Our study extends the sex-specific regulation of these energy-regulating pathways
280 to the neocortex.

281

282 ***Importance of biological sex on the impact of food restriction on cortical function.***

283 Food restriction protocols are widely used to motivate animals in behavioural studies examining
284 cortical function[15–17]. Our findings suggest that these protocols are likely to have greater impacts on
285 basal neocortical function in males, as compared to females. Consistent with this, a recent study has
286 found that food restriction in juvenile mice strongly impacts cognitive flexibility in learning and
287 decision-making in adulthood, specifically for males but not females[47,48]. Such sex-specific impacts of
288 food restriction on neocortical function are important to take into consideration in the design and
289 interpretation of such studies.

290 Diet is known to have a considerable impact on neurological diseases, including epilepsy,
291 Alzheimer's disease, and other neurodegenerative diseases[49,50]. Whilst calorie restricted diets have
292 proven to be of benefit in this regard, the sex-dependency of such interventions have not been
293 thoroughly investigated, though on the basis of our findings it is conceivable that males and females
294 may respond differently to dietary interventions. The inclusion of both males and females in
295 biomedical research, and the study of sex differences, is therefore of considerable importance for
296 ensuring efficacious treatments are developed for both sexes.

297 In conclusion, we find that visual cortical coding and energy usage in females are resistant to
298 food restriction, in contrast to males. Our findings establish that sex-specific adaptations in energy
299 usage, previously described in peripheral tissue under metabolic challenge, extends to the neocortex.

Acknowledgments

We thank the GENIE Program and the Janelia Research Campus (V. Jayaraman, R. Kerr, D. Kim, L. Looger, and K. Svoboda) for making GCaMP6 available. We thank J. Hirrlinger (Carl Ludwig Institute of Physiology, University of Leipzig, Germany) for providing the ATeam1.03^{YEMK} mouse line. We thank Sang Seo and Aditi Singh for assistance and guidance in RNA sequencing and analysis. We thank Will Cawthorn for discussions on the manuscript. This work was funded by the BBSRC (Responsive Mode Research Grant (BB/T007907/1 to N.R. and Z.P.), the Royal Commission for the Exhibition of 1851 (research fellowship to Z.P.), the MRC (G116854; Career Development Fellowship to Z.P.), the Wellcome Trust and the Royal Society (Sir Henry Dale fellowship to N.R.), the Shirley Foundation, the Patrick Wild Centre, the RS MacDonald Charitable Trust Seedcorn Grants (to N.R. and Z.P.), the Simons Initiative for the Developing Brain (to N.R. and D.K.) and the Wellcome Trust-University of Edinburgh Institutional Strategic Support Fund (ISSF3) (to N.R.). This project has received funding from the European Research Council (ERC) under the European Union's Horizon 2020 research and innovation programme (grant agreement No. 866386).

Author contributions

Z.P. and N.R. designed the experiments. Z.P. performed and analysed calcium imaging experiments and ELISAs. D.K. performed and analysed calcium and ATP imaging experiments. Z.P. and M.R. and E.O. processed tissue for RNA sequencing and analyzed data. P.M. performed and analyzed ELISAs. N.R. supervised the project. Z.P. and N.R. wrote the manuscript with input from all authors.

Declaration of Interests

The authors declare no competing interests.

Inclusion and Diversity

One or more of the authors of this paper self-identifies as an underrepresented ethnic minority in science. One or more of the authors of this paper self-identifies as a member of the LGBTQ+ community. While citing references scientifically relevant for this work, we also actively worked to promote gender balance in our reference list.

Figure Legends

332 **Figure 1. Sex-specific impact of food restriction on weight loss and serum leptin.** (A) Animal weight
333 across time. (B) Daily food intake (two-way ANOVA: CTR male vs FR male; $t = 4.81$; $df = 25$; $p < 0.0001$;
334 CTR male vs. CTR female; $t = 0.013$; $df = 25$; $p = 0.99$; CTR female vs. FR female; $t = 6.59$; $df=25$; $p < 0.$
335 0001; FR male vs. FR female; $t = 1.93$; $df = 25$; $p = 0.07$; n = 8 CTR males, 8 FR males, 7 CTR females,
336 and 7 FR females). Percent reduction of food intake for food restriction is shown in red for each sex.
337 (C) Animal weight (two-way ANOVA: CTR male vs FR male; $t = 11.36$; $df = 25$; $p < 0.0001$; CTR female
338 vs FR female; $t = 8.36$; $df = 25$; $p < 0.0001$; n = 17 CTR males and 19 FR males; 23 CTR females and 11
339 FR females). (D) Serum leptin levels (two-way ANOVA: CTR male vs FR male; $t = 4.58$; $df = 66$; $p <$
340 0.0001; CTR females vs FR females; $t = 1.00$; $df = 66$; $p = 0.32$; n = 17 CTR males and 19 FR males; 23
341 CTR females and 11 FR females). (E) Left. AMPK Thr172 phosphorylation, normalized by total AMPK,
342 in primary visual cortex (V1) tissue (two-way ANOVA: CTR male vs FR male; $t = 2.28$; $df = 39$; $p = 0.022$;
343 CTR female vs. FR female; $t = 0.64$; $df = 39$; $p = 0.11$; n = 11 CTR males, 15 FR males, 11 CTR females,
344 and 6 FR females). Right. PPARα activity in V1 tissue, as assessed by levels of DNA binding, normalized
345 to protein level (two-way ANOVA: CTR male vs FR male; $t = 4.81$; $df = 30$; $p = 0.013$; CTR female vs. FR
346 female; $t = 0.0016$; $df = 30$; $p = 0.99$; n = 5 CTR males, 11 FR males, n = 9 CTR females, and 9 FR
347 females). ***$p < 0.0001$; *$p < 0.05$; n.s. = not significant. Error bars are S.E.M.
348
349 **Figure 2. Cellular energy-regulating pathways are more robustly impacted by food restriction in**
350 **males than in females.** (A) Schema of RNA sequencing of V1 tissue. (B) Volcano plot of fold change
351 expression with food restriction vs. significance for all analyzed genes; broken horizontal line denotes
352 adjusted $p \leq 0.1$ significance level, below which non-significantly regulated expressed genes are
353 marked by grey. Inset: Venn diagram showing the number of significantly differentially expressed
354 genes with food restriction in males and females. (C) Gene Set Enrichment Analysis using Hallmark
355 Gene Sets, depicted using a volcano plot of Enrichment Score vs. significance for males (left) and
356 females (right); broken horizontal lines denotes adjusted $p < 0.05$ significance level. Inset: Venn
357 diagram showing the number of significantly regulated gene sets with food restriction in males and
358 females. (D) Complete list of significantly enriched gene sets by food-restriction in males and females
359 for analysis in C. Gene sets of interest are denoted by a box (oxidative phosphorylation: male; $t = 0.48$;
360 $p < 0.0001$; female; $t = -0.17$; $p = 0.96$; mTORC1 signaling: male; $t = 0.46$; $p < 0.0001$; female; $t = -0.18$;
361 $p = 0.98$; fatty acid metabolism: male; $t = 0.43$; $p < 0.0001$; $t = 0.2$; $p = 0.88$; PI3K/AKT/mTOR signaling:
362 male; $t = 0.34$; $p = 0.027$; female; $t = 0.17$; $p = 0.98$). All data from 4 CTR males, 4 FR males, 4 CTR
363 females, and 4 FR females.
364

365 **Figure 3. ATP usage and orientation selectivity in V1 are more robustly decreased by food restriction**
366 **in males than in females.** (A) Schemata of ATP imaging experiment. Top: example field of view of V1
367 layer 2/3 neurons in the ATeam1.03^{YEMK} transgenic mouse (scale bar: 10 µm). Bottom: ATP synthesis
368 inhibitors were used to isolate ATP usage, recorded as a decrease in FRET signal during presentation
369 of natural, outdoor scenes. (B) Normalized ATeam1.03^{YEMK} FRET signal in males and during
370 presentation of natural, outdoor scenes. ATP synthesis inhibitors (arrow) were added to isolate ATP
371 usage. Inset: Time to 50% decay of the ATeam1.03^{YEMK} FRET signal (two-way ANOVA: t = 2.87; df = 37;
372 p = 0. 0067; n = 11 CTR males and 10 FR males). (C) As in (B) but for females (inset: two-way ANOVA:
373 t = 1.36; df = 37; p = 0.18; n = 12 CTR females and n = 8 FR females). (D) Top: Schema of two-photon
374 imaging and sample field of view of V1 layer 2/3 neurons expressing GCaMP6s (scale bar: 10 µm).
375 Bottom: Sample fluorescent signals (grey) from a selected neuron (black circle) in response to 6
376 drifting gratings of varying orientations. Trial averages are in black. Horizontal bar denotes 2s grating
377 presentation. (E) Mean orientation tuning curves normalized to the response to the preferred
378 orientation for CTR and FR males (data from [13]). Note that -90° and +90° conditions correspond to the
379 same visual stimulus. Inset: Orientation selectivity index (OSI; two-way ANOVA: t = 3.75; df = 27; p =
380 0.0009 n = 8 CTR and 8 FR males). (F) As in (E) but for females (Inset: two-way ANOVA: t = 1.90; df =
381 27; p = 0.08; n = 7 CTR females and 9 FR females). **p < 0.01; ***p < 0.001; n.s. = not significant. Error
382 bars are S.E.M. Data from male mice are from a previously published dataset obtained under similar
383 conditions[13].
384
385 **Supplemental Figure 1. ATP usage in visual cortex is not affected by food restriction in the absence**
386 **of visual stimulation.** (A) Schemata of ATP imaging experiment in the absence of visual stimulation
387 (dark screen). Top: example field of view of V1 layer 2/3 neurons in the ATeam1.03^{YEMK} transgenic
388 mouse (scale bar: 10 µm). Bottom: ATP synthesis inhibitors were used to isolate ATP usage, recorded
389 as a decrease in FRET signal. (B) Normalized ATeam1.03^{YEMK} FRET signal in males in the absence of
390 visual stimulation (dark screen). ATP synthesis inhibitors (arrow) were added to isolate ATP usage.
391 Inset: Time to 50% decay of the ATeam1.03^{YEMK} FRET signal (two-way ANOVA: t = 0.14; df = 24; p = 0.
392 89; n = 8 CTR males and 6 FR males). (C) As in (B) but for females (inset: two-way ANOVA: t = 0.64; df
393 = 37; p = 0.52; n = 8 CTR females and n = 8 FR females). n.s. = not significant. Error bars are S.E.M.
394
395 **Supplemental Figure 2. Pupil diameter during visual stimulation is not affected by sex or food**
396 **restriction.** (A) Top: Sample camera image of pupil (red outline) during visual stimulation. Bottom:
397 Pupil diameter during the presentation of drifting gratings. (B) Pupil diameter was comparable across
398 sex and diet. To assess significance across sex, pupil data within a sex was pooled (across diet) (t-test:
399 Male vs Female; t = 0.82; df = 18; p = 0.42; n = 7 CTR males, 8 FR females, 1 CTR female, and 4 FR

400 females). n.s. = not significant. Error bars are S.E.M. Data from male mice are from a previously
401 published dataset obtained under similar conditions[13].
402
403 **Supplemental Figure 3. Bayes factor analysis reveals statistically robust impact of metabolic stress**
404 **on V1 energy usage and visual coding in males, but not in females.** Bayes factor (BF_{10}) along with
405 quantified effect size and 95% confidence intervals (CI) are shown for males (green) and females
406 (purple). Across parameters, BF_{10} and effect sizes are greater for males than females, meaning that
407 food restriction induces a more robust effect on visual cortical function and energy usage in males
408 than females.
409
410
411 # STAR METHODS
412
413 ## RESOURCE AVAILABILITY
414
415 ### *Lead contact*
416 Further information and requests for resources and materials should be directed to and will be fulfilled
417 by the lead contact Nathalie L. Rochefort (n.rochefort@ed.ac.uk).
418
419 ### *Materials availability*
420 This study did not generate new unique reagents.
421
422 ### *Data and code availability*
423 1. GEO accession number for RNA-seq datasets: GSE233435
424 2. Processed data will be made available at https://datashare.ed.ac.uk/handle/10283/3871.
425 Requests for raw data should be made to and will be fulfilled by the lead contact
426 (n.rochefort@ed.ac.uk).
427 3. MATLAB scripts to analyse data have been previously published[13] and are available at
428 https://zenodo.org/record/5561795#.YmJ3AtrMJPY and https://github.com/rochefort-
429 lab/Padamsey-et-al-Neuron-2022.
430 4. Any additional information required to reanalyze the data reported in this paper is available
431 from the lead contact upon request.

432

433 **EXPERIMENTAL MODEL AND SUBJECT DETAILS**

434 Experiments were approved by the University of Edinburgh's Animal Welfare and Ethical Review Board
435 (AWERB) and carried out under Home Office (UK) approved project and personal licenses. All
436 experiments conformed to the UK Animals (Scientific Procedures) Act 1986 and the European
437 Directive 86/609/EEC and 2010/63/EU on the protection of animals used for experimental purposes.

438

439 This study used male and female C57BL/6J mice (RRID:IMSR_JAX:000664; Jackson Laboratory) and
440 male B6-Tg (Thy1.2-ATeam1.03^{YEMK})^{AJhi} transgenic mice, that were bred on a C57BL/6J background
441 (RRID:MGI:5882597; https://scicrunch.org/resources). Animals were group housed (2-5 animals/cage)
442 and maintained on a reverse light/dark (12h/12h) cycle in a room kept at 21±2°C and 55±10%
443 humidity.

444

445 For data associated with *in vivo* recordings (Figure 3), data obtained in female mice were compared
446 to our previously published datasets obtained under similar conditions in male mice[13]

447

448 **METHOD DETAILS**

449

450 **Food restriction**

451 Mice (7-9 weeks of age) either had *ad libitum* access to food (RM1 expanded pellets; DBM Scotland
452 UK) or were food restricted for 2-3 weeks to 85% of their baseline bodyweight prior to
453 experimentation as previously described[13]. Briefly, for food restriction, one ration of food was given
454 4-8 hours prior to the end of the dark cycle, with the amount of food progressively reduced to achieve
455 target weight. 1-2 hour prior to experimentation, all animals had *ad libitum* access to food until sated.

456

457 **AAV injection and cranial window**

458 For calcium imaging experiments, C57BL6 were anesthetized using isoflurane, and given pre-operative
459 analgesia (vetergesic: 0.1 mg/kg; carprieve: 5 mg/kg; rapidexon: 2 mg/kg) along with warm Ringer's
460 solution (25ml/kg) subcutaneously; vetergesic jelly was additionally given orally post-operatively 24
461 hours later. Opaque eye cream was applied to the eyes (Bepanthen, Bayer, Germany). A craniotomy
462 (2x2 mm) was applied over left V1 (centre at 2.5 mm mediolateral and 0.5 mm anterior to lambda).
463 Flexed GCaMP6S (AAV1.Syn.Flex.GCaMP6s.WPRE.SV40; Addgene; RRID:Addgene_105558-AAV1)
464 diluted 1:10 in saline, along with CaMKII-dependent Cre-recombinase (AAV1.CamKII 0.4.Cre.SV40;
465 Addgene; RRID:Addgene_105558-AAV1) diluted 1:100 saline was injected at the centre of the

466 craniotomy via a sharp glass pipette. Injections were targeted to layer 2/3, with 100 nL of virus solution
467 injected (2.5nL/30s) at each of 3 depths (150, 250 and 350 µm) via a sharp glass pipette using a
468 Nanoject III (Drummond Scientific). A glass window was then used to seal the craniotomy, and
469 superglued in place. The window was made of 1 or 2 glass coverslips (Menzel-Glaser # 0), in the latter
470 case the 2 cover slips were glued together with optically-clear, UV-cured glue (Norland Optical
471 Adhesive no. 60); the inner window was 2.0 mm x 2.0 mm, the outer window was 2.5 mm x 2.5 mm.
472 A metal headplate was then fixed to the skull with super glue and dental cement (Paladur, Heraeus
473 Kuzler). It took 3-6 weeks for viral expression prior to experimentation.
474
475 For ATP imaging experiments, we used ATeam1.03^{YEMK} mice (RRID:MGI:5882597;
476 https://scicrunch.org/resources) that express a FRET-based sensor under the Thy1 promoter[33]. One
477 the day of experimentation, animals were anesthetized with isoflurane and given pre-operative
478 analgesia (Carprieve: 5 mg/kg) and 25 mL/kg of warm Ringer's solution subcutaneously. A headplate
479 was first fixed to the skull with superglue and dental cement, after which a small craniotomy (~0.5 x
480 ~0.5 mm) was made over left V1 (centre at 2.5 mm mediolateral and 0.5 mm anterior to lambda),
481 which was covered with agarose (1-2%) and silicone. Following recovery from anaesthesia (30-60
482 minutes) the animal was head-fixed; the agarose and silicone were removed and replaced with HEPES-
483 buffered ACSF (in mM: 124 NaCl, 20 Glucose, 10 HEPES, 2.5 KCl, 1.2 NaH_2PO_4, 2 $CaCl_2$, and 1 $CaCl_2$; pH
484 7.2-7.4).
485
486 **Habituation and Head-fixation**
487 During imaging, mice were placed in a cardboard tube and head fixed. Prior to the imaging day, mice
488 were handled daily for 2-3 weeks prior, and exposed to cardboard tubes, similar to the one on the
489 experimental rig. They were also habituated to the rig via once daily, 10-15 minute sessions for 2 days
490 prior to recording. For ATP imaging, mice were habituated to the experimental setup without head
491 fixation (10-15 min session/day for 1-2 days).
492
493 ***In vivo* two-photon imaging**
494 ATP and calcium imaging were using a two-photon resonant scanning microscope, as previously
495 described[51–53], which was equipped with a Ti:Sapphire laser (Charmeleon Vision-S, Coherent, CA) and
496 GaAsP photomultiplier tubes (Scientifica), and controlled with LabView (v8.2; National Instruments,
497 UK). Time-series xy images were acquired at 40Hz using a 25x water-immersion objective (Nikon;
498 CF175 Apo 25XC W; 1.1 NA) at depths between 160 and 280 µm below the pia. For GCaMP6s imaging,
499 excitation was tuned to 920nm. For ATP imaging (CFP/YFP FRET sensor), the laser was tuned to 850

500 nm for CFP excitation. CFP and YFP fluorescence were recorded simultaneously using a 515nm long-
501 pass dichroic mirror with the following emission filters: 485/70nm for CFP and 535/45nm for YFP
502 (mirror and filter set: T515lpxr C156624; Scientifica). Imaging data were acquired during the
503 presentation of visual stimuli, with at least 10 replicate trials for each visual stimulus. For ATP imaging,
504 three trials were taken at baseline, then ACSF containing ATP synthesis inhibitors (1 mM oligomycin
505 and 20 mM sodium iodoacetate) was applied over the open craniotomy isolate ATP usage. Thirty trials
506 were successively performed immediately after drug application. For in vivo recordings, data obtained
507 in females were compared to our previously published datasets obtained under similar conditions in
508 male mice[13].
509
510 **Visual Stimuli**
511 MATLAB (Mathworks; RRID:SCR_001622; Psychophysics Toolbox; RRID:SCR_002881) was used to
512 generate drifting grating stimuli. These were displayed on an LCD monitor (51 x 29 cm; Dell) placed 20
513 cm from the right eye, contralateral to the hemisphere with the cranial window. For food restriction
514 experiments, on a given trial, 12 full-field drifting gratings (drift angle: 0, 30, 60, 90, 120, 180, 210,
515 240, 270, 300, 330°; temporal frequency = 1 Hz), 2 s in duration, were presented in random order,
516 interspersed with grey screens (4 s duration). Gratings within a trial were randomly assigned one
517 common spatial frequency (0.02, 0.04, 0.16, or 0.32 cpd). For natural stimuli, a 60s movie was
518 presented of an outdoor movie of movement through a field and vegetation. For dark conditions, no
519 visual stimulus was presented (screen off) and all sources of light were switched off.

520 **Pupil measurements**
521 In some experiments the pupil was monitored using a USB camera (USB 2.0 monochrome camera;
522 ImagingSource) with frames captured at 30 Hz.

523 **Serum leptin measurements**
524 Serum leptin levels were analyzed using ELISA kits (Mouse Leptin Quantikine Elisa Kit, R&D Systems,
525 USA) according to manufacturer's instruction. For serum collection, trunk blood was collected from
526 mice that were briefly anesthetized (isoflurane) prior to decapitation. Blood was allowed to clot at
527 room temperature for 1-2 hours and then centrifuged for 20 minutes at 2000 x g. The serum was
528 drawn off and stored at -80°C until used.
529
530 **AMPK and PPARα measurements**
531 Levels of total AMPK, phosphorylated AMPK (Thr172), and nuclear PPARα in V1 were measured using
532 ELISA kits according to manufacturer's instructions (total AMPK: ab181422, Abcam, UK;
533 phosphorylated AMPK: KHO0651, ThermoFisher, UK; PPARα: ab133107, Abcam, UK). For tissue

534 collection, mice were briefly anesthetized (isoflurane) and decapitated. The visual cortex was
535 dissected out, snap frozen using dry ice, and stored at -80°C until used.
536
537 **RNA sequencing**
538 Bulk RNA sequencing was performed on V1. V1 tissue was collected and snap frozen from mice that
539 were briefly anesthetized (isoflurane) and decapitated. Tissue was homogenized using a bead mill
540 (Bead Mill 24, Fisher Scientific) and RNA was isolated using an RNeasy kit (Qiagen) according to
541 manufacturer's instructions. RNA integrity was confirmed (RIN > 7) and mRNA was sequenced at the
542 Oxford Genomics Centre using Illumina NovaSeq 6000.

543 **QUANTIFICATION AND STATISTICAL ANALYSIS**

544 **Ca^{2+} Imaging Analysis**
545 Image analysis for calcium imaging was performed as previously described[45,47,49]. For motion correct,
546 a discrete Fourier 2D-based image alignment was used (SIMA 1.3.2)[53]. Regions of interest (ROI) were
547 manually drawn around imaged neuronal soma using ImageJ software (NIH public domain;
548 RRID:SCR_002285). Pixel fluorescence was then averaged within each ROI to generate a time series.
549 For each ROI, baseline fluorescence (F_0) was calculated by taking the 5th percentile of the smoothed
550 time series (1 Hz lowpass, zero-phase, 60th-order FIR filter). ΔF/F was then calculated as ($F-F_0/F_0$). FISSA
551 was used to decontaminate the neuropil[55]. Subsequent analyses were performed using custom scripts
552 in MATLAB (MathWorks)[13].
553
554 **Drifting grating analysis**
555 The visual response to drifting gratings was defined as the highest mean ΔF/F, averaged within a 2s
556 window, that occurred within a 4 s window (comprising the 2s grating presentation plus the 2 s of the
557 grey screen presentation which immediately followed the grating presentation). The visual response
558 was subtracted by baseline ΔF/F, defined as the mean value within a 1 s window prior to the visual
559 response.
560
561 Responses to gratings of the same angle, but different drift directions were averaged together. Given
562 that multiple spatial frequencies were used, only the spatial frequency with the largest response,
563 meaned across all orientations, was selected for each neuron for subsequent analyses. A neuron's
564 preferred orientation was that which evoked the largest mean response.
565

Grating responsive neurons were defined as those for which grating responses were better fit with a double Gaussian curve (direction responses) than with a flat line at zero (null model), which was determined using Bayesian Information Criterion (BIC)[13]. The double Gaussian curve was defined as:

$$R(\theta) = C + R_p e^{\frac{-ang_{dir}(\theta-\theta_{pref})^2}{2\sigma^2}} + R_n e^{\frac{-ang_{dir}(\theta-\theta_{pref})^2}{2\sigma^2}}$$

Where R (θ) is the response at a given direction angle θ, C is an offset, R_p is the response to the preferred direction after subtracting the offset, θ_{pref} is the angle of the preferred direction, R_n is the response to the null direction after subtracting the offset, and $ang_{dir}(x) = \min(x, x-360, x+360)$, which constrains angular differences to 0-180°, and σ is the standard deviation of the curve.

BIC was given by:

$$BIC = nln(\overline{\sigma^2}) + kln(n)$$

Where n is the number of responses, $\overline{\sigma^2}$ is the mean residual sum of squares of the model, and k is the number of free parameters used by the model, which was zero in the case of the null model. A neuron was considered significantly grating-responsive if the BIC_{null} - $BIC_{Gaussian} \geq 10$, which provides strong evidence against the null model[54].

Orientation selectivity

The orientation selectivity index (OSI) of grating-responsive neurons was calculated as:

$$OSI = 1 - CirVar = abs\left(\frac{\sum_k R(\theta_k)e^{2i\theta_k}}{\sum_k R(\theta_k)}\right)$$

Where *Cirvar* is the circular variance and R (θ_k) is the mean response to the k_{th} angle θ in orientation space, averaged across direction (see detailed description in [55]). Mean responses less than zero were set to zero. We used the median OSI values across neurons within an animal.

Direction selectivity

The direction selectivity index (DSI) of grating-responsive neurons was calculated as:

599 $$DSI = 1 - dirCirVar = abs\left(\frac{\sum_k R(\theta_k)e^{i\theta_k}}{\sum_k R(\theta_k)}\right)$$

600

601 Where *dirCirVar* is the circular variance in direction space and R (θ_k) is the mean response to the k_{th}
602 angle θ in direction space (see detailed description in [55]). Mean responses less than zero were set to
603 zero. We used the median DSI values across neurons within an animal.

604

605 **Pupil Analysis**

606 Pupil diameter was quantified with custom scripts in MATLAB using functions from the Imaging
607 Processing Toolbox, namely:

608 1) *imresize* to resize the video
609 2) *medfilt2* and *imadjust* to remove noise and adjust contrast
610 3) *imbinarize, imclearborder,* and *bwpropfilt* to find the pupil
611 4) *regionprops* to fit an ellipsoid around the pupil

612 The pupil diameter (d) was calculated from the fitted ellipsoid as:

613 $$d = 2\sqrt{\text{semi-major axis} * \text{semi-minor axis}}$$

614 **ATP measurements**

615 For ATeam1.03[YEMK] imaging, CFP and YFP fluorescence was averaged across ROIs drawn around visible
616 soma in the field of view, after background subtraction. FRET was calculated as a ratio of YFP/CFP
617 fluorescence, and decayed as a function of time with visual stimulation in the presence of ATP
618 synthesis inhibitors. The FRET signal was bound between 0 and 1 by first subtracting the mean FRET
619 signal during the last 3 imaging trials (the FRET signal plateaued at this point), and then dividing by the
620 mean FRET signal at baseline. The FRET decay half time was defined as the time required for the FRET
621 to decay to 50% of its baseline value.

622

623 **Differential gene expression analysis**

624 RNA sequencing reads were mapped, using STAR 2.4.oi, to the *Mus musculus* primary assembly
625 (Ensembl v80)[56]. FeatureCounts 1.4.6-p2 was used to count reads uniquely aligned to annotated
626 genes[57]. Differential gene expression analysis was then conducted using DESeq2 1.12.4 (betaPrior =
627 False) to normalize counts[60]. For each gene, a fold change in gene expression was defined as
628 $log_2 \frac{\text{Normalized count under food restriction (FR)}}{\text{Normalized count under control conditions (CTR)}}$ for males and females. Gene set enrichment analysis
629 (GSEA) was conducted using GSEA software (https://www.gsea-msigdb.org/gsea/index.jsp) using the
630 Hallmarks Gene Sets (v7.5.1).

631

632 **Statistics**

633 Statistical tests, p values, and the number and definition of independent units are stated in the figure
634 legends. For all measures, the number of animals was taken as the statically independent unit. Sample
635 size was determined by *a priori* based on calculations, with an aim of achieving 80% power on the
636 basis of a 20% group difference and a significance threshold of $p < 0.05$. Averages are means, except
637 where indicated. Group means and variances were taken from pilot data or previously published
638 data[13]. Where applicable, ANOVA was used to assess significance, followed by *post-hoc* Fisher LSD
639 tests to prevent loss of power. Statistical tests were carried out in Prism 6 (GraphPad Prism;
640 RRID:SCR_002798). Averages denoted in figures represent means, with error bars representing the
641 standard error of the means (S.E.M.). We complemented our statistical analyses using Bayes factor
642 hypothesis testing (Supplemental Figure 3) as described in[35,36] using JASP software to calculates Bayes
643 factor, effect size, and confidence intervals (https://jasp-stats.org/). As recommended, we used a
644 default, Cauchy distribution with a spread of $1/\sqrt{2}$ as a prior distribution of effect size. A $BF_{10} < 0.33$ is
645 considered to be moderate evidence for the absence of an effect[35,36].

646

647 ## Declaration of interests

648 The authors declare no competing interests.

649

650 ## References

651 1. Andersson B, Xu XF, Rebuffé-Scrive M, Terning K, Krotkiewski M, Björntorp P. The effects of
652 exercise, training on body composition and metabolism in men and women. *Int J Obes*.
653 1991;15(1):75-81.
654 2. Cortright RN, Koves TR. Sex Differences in Substrate Metabolism and Energy Homeostasis.
655 *Can J Appl Physiol*. 2000;25(4):288-311.
656 3. Volek J, Sharman M, Gómez A, et al. Comparison of energy-restricted very low-carbohydrate
657 and low-fat diets on weight loss and body composition in overweight men and women. *Nutr*
658 *Metab (Lond)*. 2004;1(1):13.
659 4. McCarthy D, Berg A. Weight Loss Strategies and the Risk of Skeletal Muscle Mass Loss.
660 *Nutrients*. 2021;13(7).
661 5. Tirosh A, De Souza RJ, Sacks F, Bray GA, Smith SR, LeBoff MS. Sex differences in the effects of
662 weight loss diets on bone mineral density and body composition: POUNDS LOST trial. *J Clin*
663 *Endocrinol Metab*. 2015;100(6):2463-2471.
664 6. Suchacki KJ, Thomas BJ, Ikushima YM, et al. The effects of caloric restriction on adipose tissue

665 and metabolic health are sex- and age-dependent. *Elife*. 2023;12.
666 7. Boutwell K, Rusch P. Some physiological effects associated with chronic caloric restriction. *Am*
667 *J Physiol*. 1948;154(3):517-524.
668 8. Ahlma RS, Prabakaran D, Mantzoros C, et al. Role of leptin in the neuroendocrine response to
669 fasting. *Nature*. 1996;382(6588):250-252.
670 9. Gill C, Rissman E. Female Sexual Behavior Is Inhibited by Short- and Long-term Food
671 Restriction. *Physiol Behav*. 1997;61(3):387-394.
672 10. Harris JJ, Jolivet R, Attwell D. Synaptic Energy Use and Supply. *Neuron*. 2012;75(5):762-777.
673 11. Attwell D, Laughlin SB. An Energy Budget for Signaling in the Grey Matter of the Brain. *J Cereb*
674 *Blood Flow Metab*. 2001;21(10):1133-1145.
675 12. Herculano-Houzel S. Scaling of Brain Metabolism with a Fixed Energy Budget per Neuron:
676 Implications for Neuronal Activity, Plasticity and Evolution. Perc M, ed. *PLoS One*.
677 2011;6(3):e17514.
678 13. Padamsey Z, Katsanevaki D, Dupuy N, Rochefort NL. Neocortex saves energy by reducing
679 coding precision during food scarcity. *Neuron*. 2022;110(2):280-296.e10.
680 14. Baile CA, Della-Fera MA, Martin RJ. Regulation of Metabolism and Body Fat Mass by Leptin.
681 *Annu Rev Nutr*. 2000;20(1):105-127.
682 15. Guo Z V, Hires SA, Li N, et al. Procedures for behavioral experiments in head-fixed mice. *PLoS*
683 *One*. 2014;9(2):e88678.
684 16. Goltstein PM, Reinert S, Glas A, Bonhoeffer T, Hübener M. Food and water restriction lead to
685 differential learning behaviors in a head-fixed two-choice visual discrimination task for mice.
686 *PLoS One*. 2018;13(9).
687 17. Toth LA, Gardiner TW. Food and Water Restriction Protocols: Physiological and Behavioral
688 Considerations. *Contemp Top Lab Anim Sci*. Published online 2000.
689 18. Burgess CR, Livneh Y, Ramesh RN, Andermann ML. Gating of visual processing by
690 physiological need. *Curr Opin Neurobiol*. 2018;49:16-23.
691 19. Burgess CR, Ramesh RN, Sugden AU, et al. Hunger-Dependent Enhancement of Food Cue
692 Responses in Mouse Postrhinal Cortex and Lateral Article Hunger-Dependent Enhancement
693 of Food Cue Responses in Mouse Postrhinal Cortex and Lateral Amygdala. *Neuron*.
694 2016;91(5):1154-1169.
695 20. Garza-Lombó C, Schroder A, Reyes-Reyes EM, Franco R. mTOR/AMPK signaling in the brain:
696 Cell metabolism, proteostasis and survival. *Curr Opin Toxicol*. 2018;8:102-110.
697 21. Dagon Y, Hur E, Zheng B, Wellenstein K, Cantley LC, Kahn BB. P70S6 kinase phosphorylates
698 AMPK on serine 491 to mediate leptin's effect on food intake. *Cell Metab*. 2012;16(1):104-

699 112.
700 22. Dagon Y, Avraham Y, Magen I, Gertler A, Ben-Hur T, Berry EM. Nutritional Status, Cognition,
701 and Survival. *J Biol Chem*. 2005;280(51):42142-42148.
702 23. Takei N, Nawa H. mTOR signaling and its roles in normal and abnormal brain development.
703 *Front Mol Neurosci*. 2014;7(1 APR):1-12.
704 24. Herzig S, Shaw RJ. AMPK: Guardian of metabolism and mitochondrial homeostasis. *Nat Rev*
705 *Mol Cell Biol*. 2018;19(2):121-135.
706 25. de la Cruz López KG, Toledo Guzmán ME, Sánchez EO, García Carrancá A. mTORC1 as a
707 Regulator of Mitochondrial Functions and a Therapeutic Target in Cancer. *Front Oncol*.
708 2019;9(December):1-22.
709 26. Unger RH, Zhou YT, Orci L. Regulation of fatty acid homeostasis in cells: Novel role of leptin.
710 *Proc Natl Acad Sci U S A*. 1999;96(5):2327-2332.
711 27. Poulsen L la C, Siersbæk M, Mandrup S. PPARs: Fatty acid sensors controlling metabolism.
712 *Semin Cell Dev Biol*. 2012;23(6):631-639.
713 28. Wójtowicz S, Strosznajder AK, Jeżyna M, Strosznajder JB. The Novel Role of PPAR Alpha in the
714 Brain: Promising Target in Therapy of Alzheimer's Disease and Other Neurodegenerative
715 Disorders. *Neurochem Res*. 2020;45(5):972-988.
716 29. Kwon O, Kim KW, Kim MS. Leptin signalling pathways in hypothalamic neurons. *Cell Mol Life*
717 *Sci*. 2016;73(7):1457-1477.
718 30. Brown LM, Clegg DJ. Central effects of estradiol in the regulation of food intake, body weight,
719 and adiposity. *J Steroid Biochem Mol Biol*. 2010;122(1-3):65-73.
720 31. Estep PW, Warner JB, Bulyk ML. Short-Term Calorie Restriction in Male Mice Feminizes Gene
721 Expression and Alters Key Regulators of Conserved Aging Regulatory Pathways. Orban L, ed.
722 *PLoS One*. 2009;4(4):e5242.
723 32. Wood SH, Dam S van, Craig T, et al. Transcriptome analysis in calorie-restricted rats
724 implicates epigenetic and post-translational mechanisms in neuroprotection and aging.
725 *Genome Biol*. 2015;16(1):1-18.
726 33. Trevisiol A, Saab AS, Winkler U, et al. Monitoring ATP dynamics in electrically active white
727 matter tracts. *Elife*. 2017;6.
728 34. Baeza-Lehnert F, Saab AS, Gutiérrez R, et al. Non-Canonical Control of Neuronal Energy Status
729 by the Na + Pump. *Cell Metab*. 2019;29(3):668-680.e4.
730 35. van Doorn J, van den Bergh D, Böhm U, et al. The JASP guidelines for conducting and
731 reporting a Bayesian analysis. *Psychon Bull Rev*. 2021;28(3):813-826.
732 36. Keysers C, Gazzola V, Wagenmakers EJ. Using Bayes factor hypothesis testing in neuroscience

733 to establish evidence of absence. *Nat Neurosci*. 2020;23(7):788-799.
734 37. Collet TH, Sonoyama T, Henning E, et al. A metabolomic signature of acute caloric restriction.
735 *J Clin Endocrinol Metab*. 2017;102(12):4486-4495.
736 38. Cuevas-Cervera M, Perez-Montilla J, Gonzalez-Muñoz A, Garcia-Rios M, Navarro-Ledesma S.
737 The Effectiveness of Intermittent Fasting, Time Restricted Feeding, Caloric Restriction, a
738 Ketogenic Diet and the Mediterranean Diet as Part of the Treatment Plan to Improve Health
739 and Chronic Musculoskeletal Pain: A Systematic Review. *Int J Environ Res Public Health*.
740 2022;19(11):6698.
741 39. Hofer SJ, Carmona-Gutierrez D, Mueller MI, Madeo F. The ups and downs of caloric
742 restriction and fasting: from molecular effects to clinical application. *EMBO Mol Med*.
743 2022;14(1).
744 40. Mitchell SJ, Madrigal-Matute J, Scheibye-Knudsen M, et al. Effects of Sex, Strain, and Energy
745 Intake on Hallmarks of Aging in Mice. *Cell Metab*. 2016;23(6):1093-1112.
746 41. Kane AE, Sinclair DA, Mitchell JR, Mitchell SJ. Sex differences in the response to dietary
747 restriction in rodents. *Curr Opin Physiol*. 2018;6:28-34.
748 42. Gao Q, Horvath TL. Cross-talk between estrogen and leptin signaling in the hypothalamus. *Am*
749 *J Physiol - Endocrinol Metab*. 2008;294(5).
750 43. Irwin RW, Yao J, Hamilton RT, Cadenas E, Brinton RD, Nilsen J. Progesterone and estrogen
751 regulate oxidative metabolism in brain mitochondria. *Endocrinology*. 2008;149(6):3167-3175.
752 44. Brinton RD. Estrogen regulation of glucose metabolism and mitochondrial function:
753 Therapeutic implications for prevention of Alzheimer's disease. *Adv Drug Deliv Rev*.
754 2008;60(13-14):1504-1511.
755 45. Baar EL, Carbajal KA, Ong IM, Lamming DW. Sex- and tissue-specific changes in mTOR
756 signaling with age in C57BL/6J mice. *Aging Cell*. 2016;15(1):155-166.
757 46. Brown KD, Waggy ED, Nair S, et al. Sex Differences in Cardiac AMP-Activated Protein Kinase
758 Following Exhaustive Exercise. *Sport Med Int Open*. 2020;4(01):E13-E18.
759 47. Clemens AM, Lenschow C, Beed P, et al. Estrus-Cycle Regulation of Cortical Inhibition. *Curr*
760 *Biol*. 2019;29(4):605-615.e6.
761 48. Lin WC, Liu C, Kosillo P, et al. Transient food insecurity during the juvenile-adolescent period
762 affects adult weight, cognitive flexibility, and dopamine neurobiology. *Curr Biol*.
763 2022;32(17):3690-3703.e5.
764 49. de Carvalho T. Calorie restriction or dietary restriction: how far they can protect the brain
765 against neurodegenerative diseases? *Neural Regen Res*. 2022;17(8):1640.
766 50. Schroeder JE, Richardson JC, Virley DJ. Dietary manipulation and caloric restriction in the

767 development of mouse models relevant to neurological diseases. *Biochim Biophys Acta - Mol*
768 *Basis Dis*. 2010;1802(10):840-846.
769 51. Pakan JM, Lowe SC, Dylda E, et al. Behavioral-state modulation of inhibition is context-
770 dependent and cell type specific in mouse visual cortex. *Elife*. 2016;5:1-18.
771 52. Pakan JMP, Currie SP, Fischer L, Rochefort NL. The Impact of Visual Cues, Reward, and Motor
772 Feedback on the Representation of Behaviorally Relevant Spatial Locations in Primary Visual
773 Cortex. *Cell Rep*. 2018;24(10):2521-2528.
774 53. Henschke JU, Dylda E, Katsanevaki D, et al. Reward Association Enhances Stimulus-Specific
775 Representations in Primary Visual Cortex. *Curr Biol*. 2020;30(10):1866-1880.e5.
776 54. Kass RE, Raftery AE. Bayes Factors. *J Am Stat Assoc*. 1995;90(430):773-795.
777 55. Mazurek M, Kager M, Van Hooser SD. Robust quantification of orientation selectivity and
778 direction selectivity. *Front Neural Circuits*. 2014;Volume 8, article 92.
779 56. Dobin A, Davis CA, Schlesinger F, et al. STAR: Ultrafast universal RNA-seq aligner.
780 *Bioinformatics*. 2013;29(1):15-21.
781 57. Liao Y, Smyth GK, Shi W. FeatureCounts: An efficient general purpose program for assigning
782 sequence reads to genomic features. *Bioinformatics*. 2014;30(7):923-930.
783

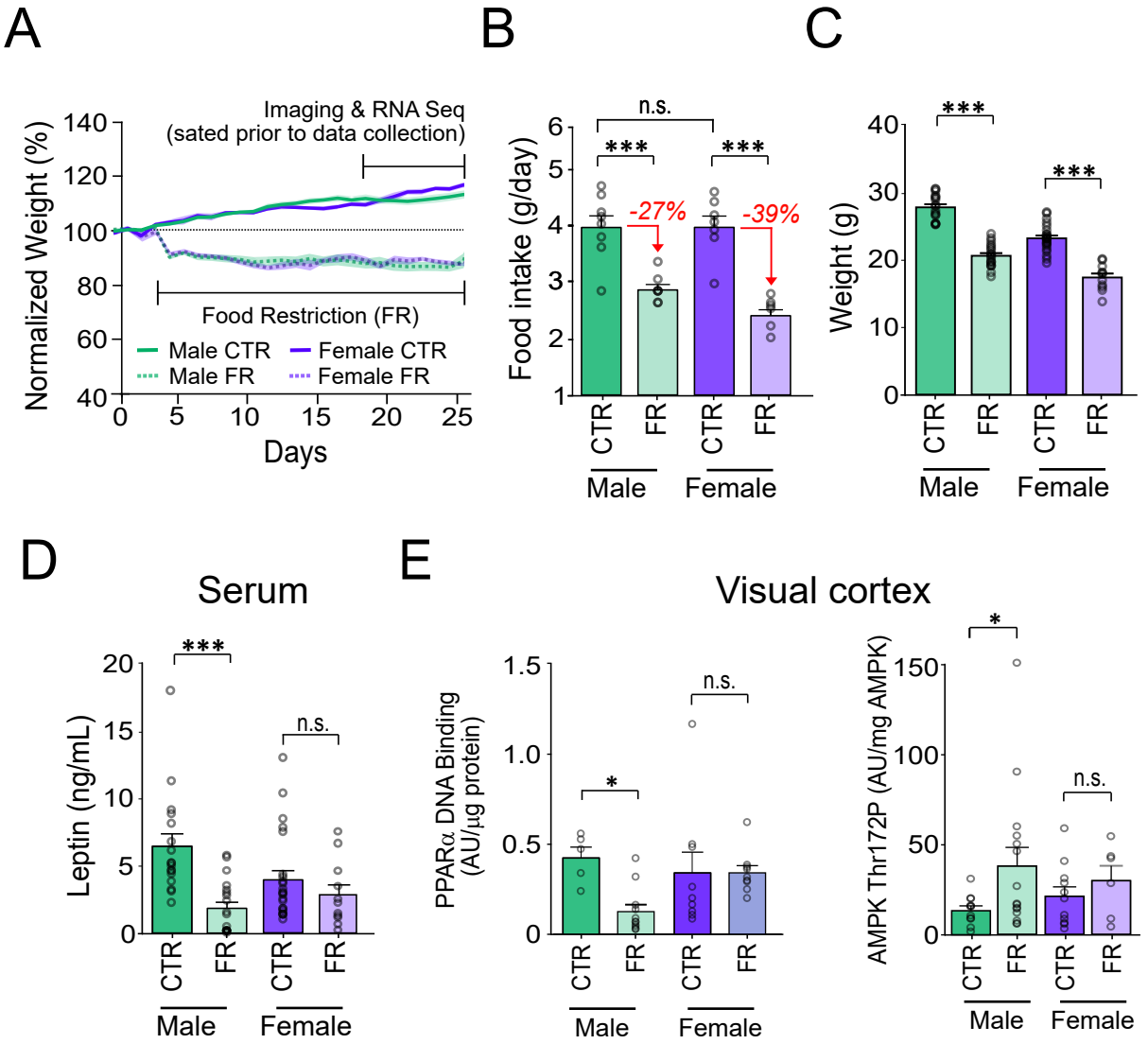
A
Imaging & RNA Seq
(sated prior to data collection)
Normalized Weight (%)
Food Restriction (FR)
Male CTR
Male FR
Female CTR
Female FR
Days
B
Food intake (g/day)
n.s.
***
***
-27%
-39%
CTR
FR
CTR
FR
Male
Female
C
Weight (g)
***
***
CTR
FR
CTR
FR
Male
Female
D
Serum
Leptin (ng/mL)
***
n.s.
CTR
FR
CTR
FR
Male
Female
E
Visual cortex
PPARα DNA Binding
(AU/µg protein)
*
n.s.
CTR
FR
CTR
FR
Male
Female
AMPK Thr172P (AU/mg AMPK)
*
n.s.
CTR
FR
CTR
FR
Male
Female

Figure 1

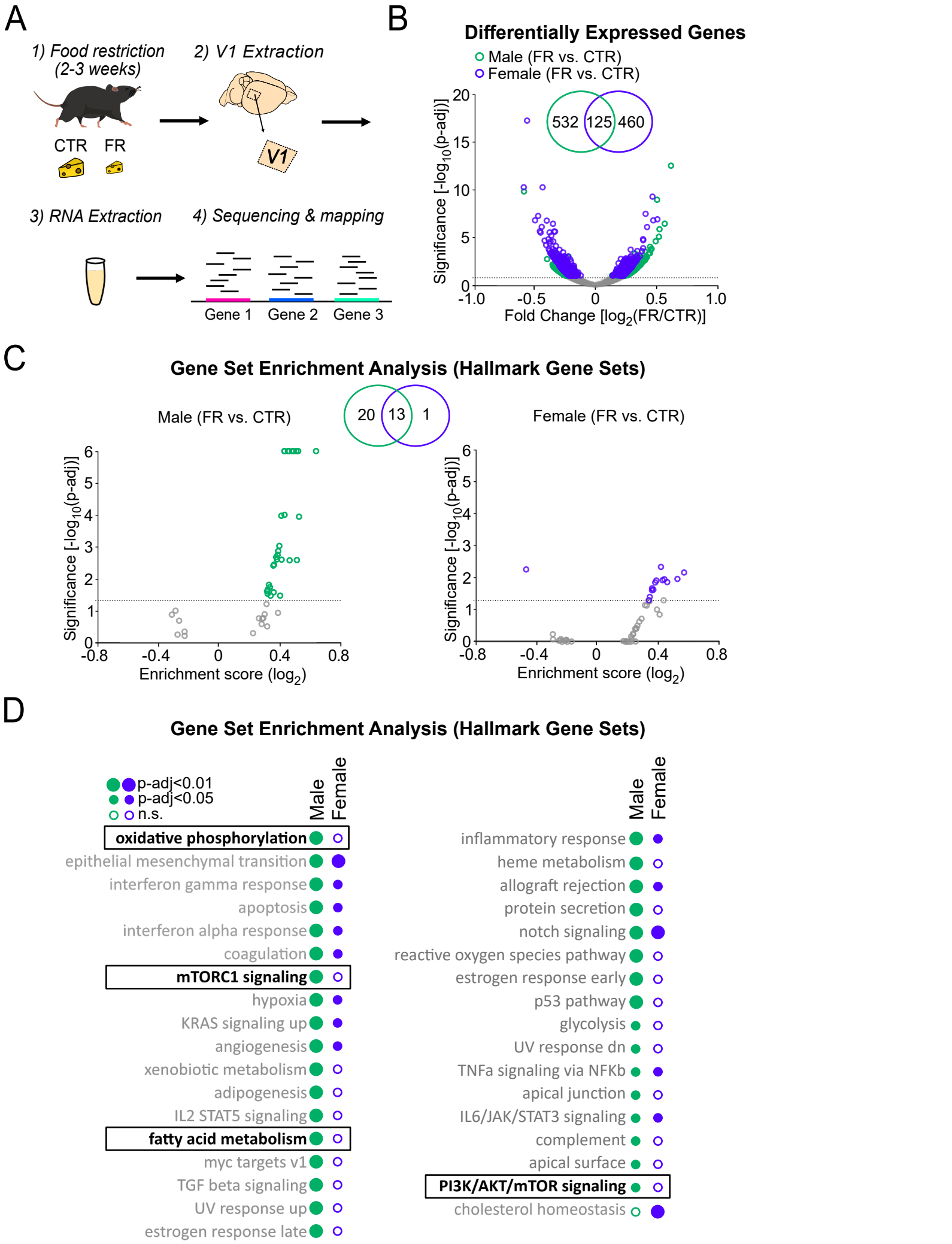
A
1) Food restriction (2-3 weeks)
2) V1 Extraction
CTR
FR
V1
3) RNA Extraction
4) Sequencing & mapping
Gene 1
Gene 2
Gene 3
B
Differentially Expressed Genes
Male (FR vs. CTR)
Female (FR vs. CTR)
532
125
460
Significance [-log10(p-adj)]
Fold Change [log2(FR/CTR)]
C
Gene Set Enrichment Analysis (Hallmark Gene Sets)
Male (FR vs. CTR)
20
13
1
Female (FR vs. CTR)
Significance [-log10(p-adj)]
Enrichment score (log2)
D
Gene Set Enrichment Analysis (Hallmark Gene Sets)
p-adj<0.01
p-adj<0.05
n.s.
Male
Female
oxidative phosphorylation
epithelial mesenchymal transition
interferon gamma response
apoptosis
interferon alpha response
coagulation
mTORC1 signaling
hypoxia
KRAS signaling up
angiogenesis
xenobiotic metabolism
adipogenesis
IL2 STAT5 signaling
fatty acid metabolism
myc targets v1
TGF beta signaling
UV response up
estrogen response late
inflammatory response
heme metabolism
allograft rejection
protein secretion
notch signaling
reactive oxygen species pathway
estrogen response early
p53 pathway
glycolysis
UV response dn
TNFa signaling via NFKb
apical junction
IL6/JAK/STAT3 signaling
complement
apical surface
PI3K/AKT/mTOR signaling
cholesterol homeostasis

Figure 2

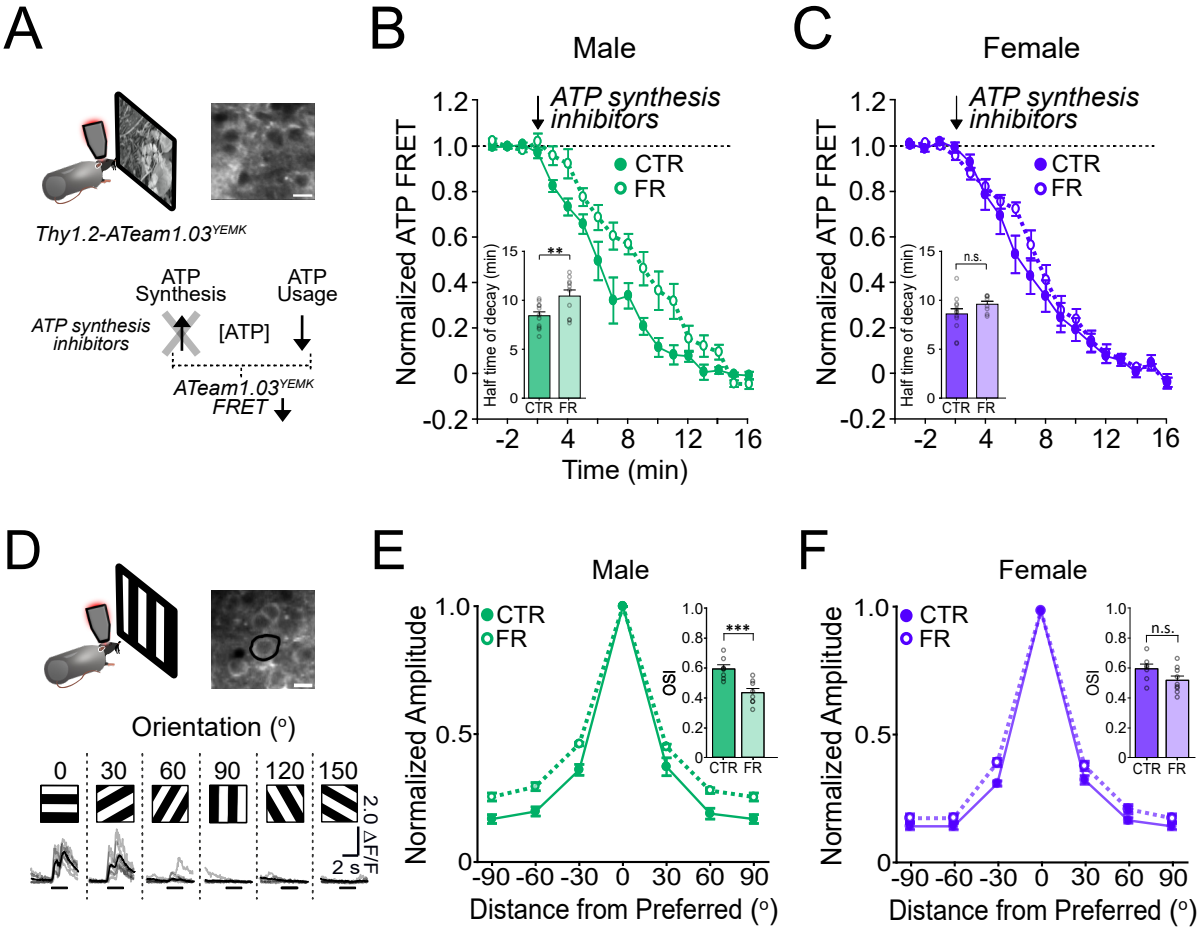
A
Thy1.2-ATeam1.03YEMK
ATP Synthesis
ATP Usage
ATP synthesis inhibitors
[ATP]
ATeam1.03YEMK FRET
B
Male
ATP synthesis inhibitors
CTR
FR
Normalized ATP FRET
Time (min)
Half time of decay (min)
**
C
Female
n.s.
D
Orientation (°)
0
30
60
90
120
150
2.0 ΔF/F
2 s
E
Male
Normalized Amplitude
Distance from Preferred (°)
OSI
***
F
Female

Figure 3

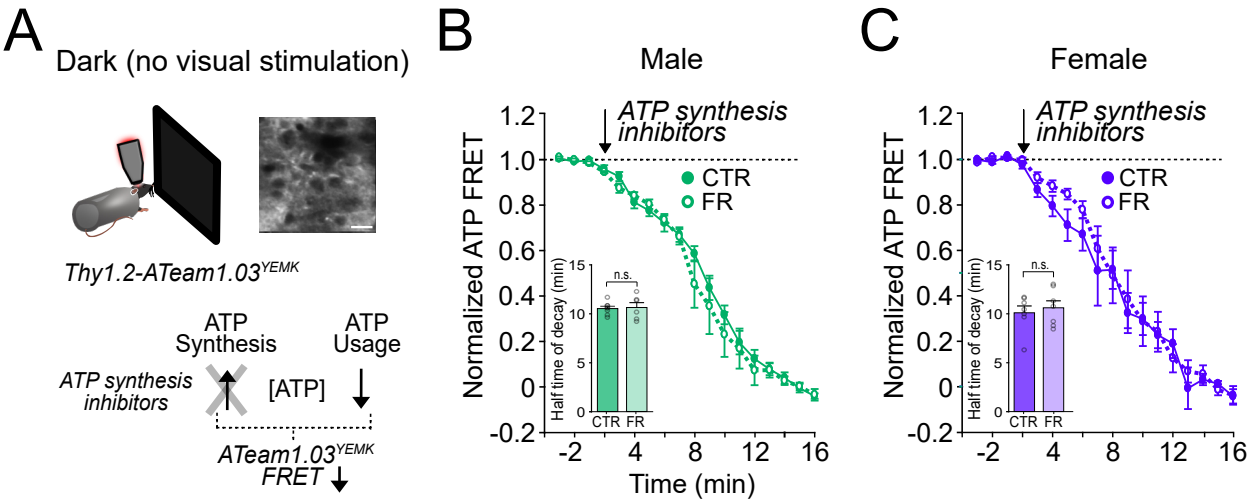

Supplemental Figure 1

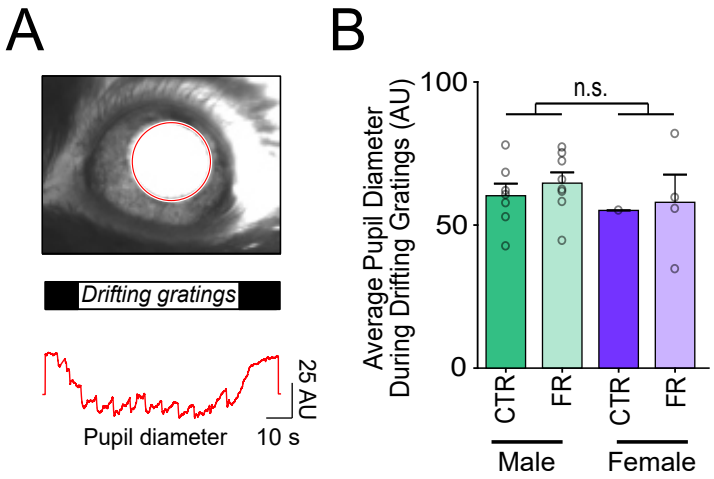

Supplemental Figure 2

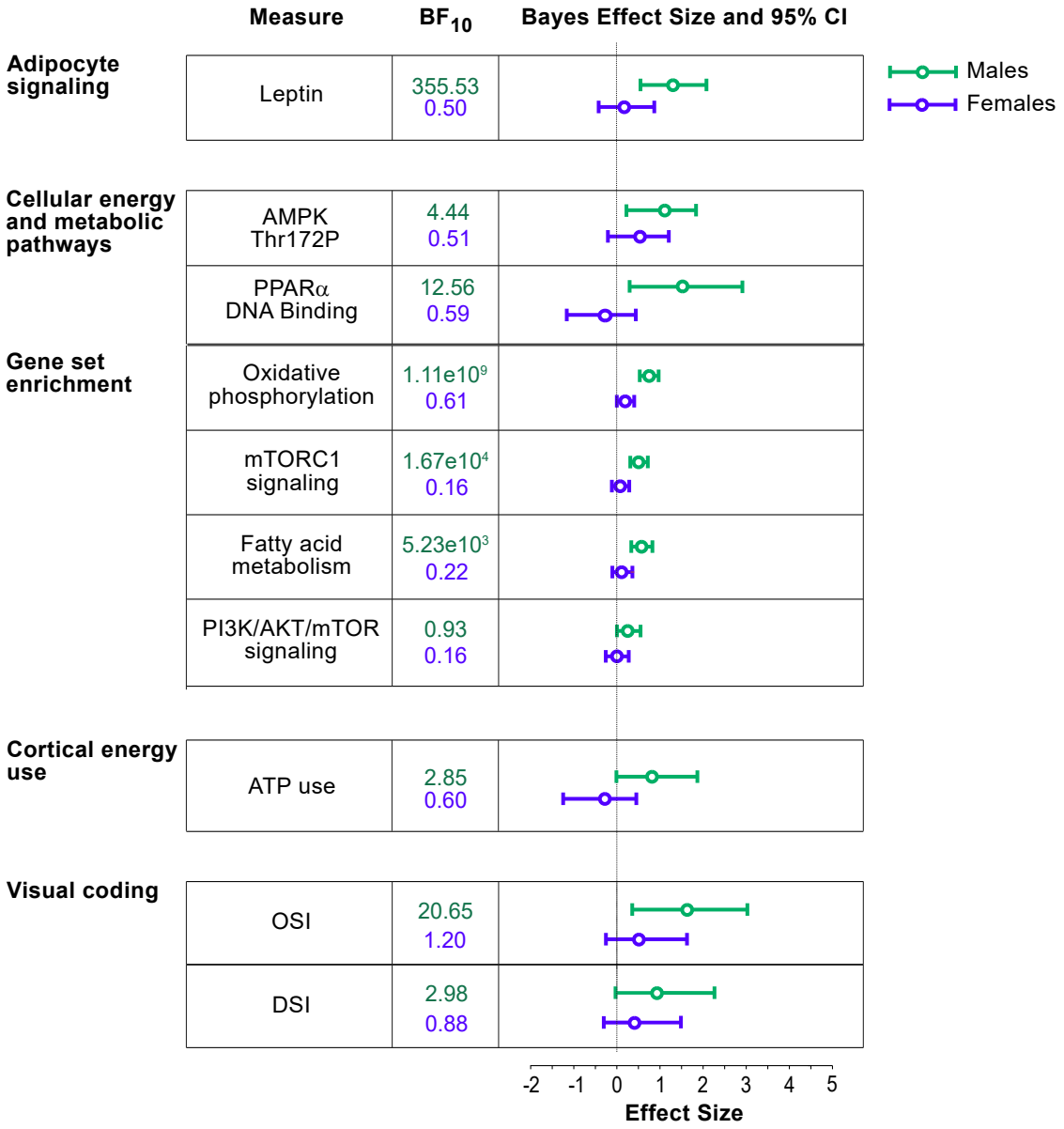

Supplemental Figure 3